ADBA Chaos and Fractals
Cutting-Edge Scientific Solutions

e-ISSN: 3023-8951
RESEARCH ARTICLE
Vol.2 / No.2 / 2025 / pp.28-37
https://doi.org/10.69882/adba.chf.2025071

Attack-Resistant Chaotic Communication System in Non-ideal Physical Channel

Timur Karimov[α,β,1], **Alexander Mikhailov**[α,2], **Vyacheslav Rybin**[α,β,3], **Varvara Sheptunova**[α,4], **Ivan Babkin**[α,β,5] **and Denis Butusov**[α,6]

[α] Computer-Aided Design Department, Saint Petersburg Electrotechnical University "LETI", 197022 Saint Petersburg, Russia, [β]Youth Research Institute, Saint Petersburg Electrotechnical University "LETI", 197022 Saint Petersburg, Russia.

ABSTRACT

Coherent chaos-based communication is a developing technique for secure data transmission based on synchronization of chaotic oscillators at the transmitter and receiver sides, which is treated as a more secure method than non-coherent communication, chaotic symbolic dynamics, and other approaches. Nowadays, digital implementation of such systems allows high precision in parameter matching and sophisticated message recovery algorithms, though challenges remain: first, in adapting chaotic signals for non-ideal physical media, e.g., acoustic channels with frequency-dependent attenuation and noise, while, second, still providing the high level of security. The current study provides the implementation of a coherent chaotic communication system based on the Sprott Case S chaotic oscillator that meets these challenges. We utilize the modulation technique, minimizing changes in chaotic dynamics that may be captured by an intruder, propose an optimization of chaotic oscillator parameters to match channel characteristics and establish a signal normalization procedure to neutralize attenuation at the receiver side. Applying spectral and return map attacks, we show that the measures taken to counteract distortion in the path do not reduce the security of the transmission. In an experiment with a physical acoustic path, we demonstrate the practical operability of our approach.

KEYWORDS

Chaos-based communication
Acoustic communication system
Secure communications
Chaotic shift keying

INTRODUCTION

Chaos-based communication is an innovative approach for secure and efficient data transmission, utilizing the distinctive features of chaotic dynamics. This type of communication is based on chaotic oscillators, which are capable of producing deterministic signals of complex, aperiodic shape, resembling noise. Unlike conventional harmonic oscillators, chaotic oscillators have several nonlinear components in feedback, which leads to their sensitivity to initial conditions and unpredictability of the trajectory in time. Such signals are irregular, aperiodic, and have a wide spectrum. That is why these oscillators are considered promising carriers of information in communication systems, enabling reliable and secure information transfer across various physical media.

One of the key discoveries in chaotic systems was the phenomenon of synchronization (Pecora and Carroll 1990; Anishchenko *et al.* 1992), that is, the signals of two identical chaotic oscillators can be fully matched when a master-slave drive between oscillators is established. Pecora and Carroll proved that a necessary condition for synchronization is the negative values of all conditional Lyapunov exponents for the slave system, which means the stability of its trajectories with respect to the master system. The Pecora-Carroll synchronization method implies a proportional control, and due to its simplicity, it is used in lots of works, demonstrating that synchronization is possible even in the case of hyperchaos (Wang *et al.* 2010), multistability (Pisarchik *et al.* 2008), delayed signals (Eisencraft *et al.* 2012), mismatch of parameters, etc.

Manuscript received: 30 June 2025,
Revised: 22 July 2025,
Accepted: 22 July 2025.

[1]tikarimov@etu.ru
[2]aamikhailov@etu.ru
[3]vgrybin@etu.ru
[4]vesheptunova@etu.ru
[5]iababkin@etu.ru
[6]dnbutusov@etu.ru (**Corresponding author**)

Chaos synchronization has become the basis for coherent chaotic communication, which assume synchronization between transmitter and receiver, in contrast to non-coherent systems, which are based on the correlation or other types of analysis for message recovery (Kaddoum 2016). Coherent systems offer a higher level of secrecy, however, they are sensitive to noise, significantly affecting the detection accuracy. Filtering or error correction techniques may be required to maintain reliable performance. In coherent systems, the simplest modulation technique is chaotic masking (Oppenheim *et al.* 1992). An information signal $m(t)$ is added to the chaotic noise-like signal of the generator on the transmitter side, and the masking signal must be subtracted at the receiving side to recover $m(t)$. Alas, the security of such modulation is weak against existing attacks. In particular, adding the message $m(t)$ to the chaotic signal alters the power of the resulting signal, which may be estimated by power analysis of the transmitted signal. Practical modulation techniques include the chaotic shift keying (CSK), first presented by Parlitz *et al.* (1992). In CSK, information bits are transmitted by selecting one of the two chaotic generator modes according to the bit stream $m(t)$. On the receiver side, two copies of the oscillator attempt to synchronize with the received signal. The copy that synchronizes more accurately indicates the bit being transmitted.

Chaotic communication can be physically implemented using both analog and digital hardware. Initially, chaotic communication systems (CCS) were proposed in analog form, e.g. in Cuomo *et al.* (1993). Nowadays, digital electronics occupy researchers interest due to its high precision, compatibility with digital data, and the ability to support complex modulation and digital signal processing algorithms. Research on novel attractors for digital CCS, modulation schemes, microcontroller or FPGA implementations, and related topics remains an active field of study (Kolumbán *et al.* 1998), Wang (2018), Babajans *et al.* (2022), Bonny *et al.* (2024), Babajans *et al.* (2025). With that, just minor quantity of studies focus on issues of chaotic communication signals propagation and adaptation for media with non-ideal properties, besides presence of additive noise. Relevant researches consider chaotic hydroacoustic path (Bai *et al.* 2019), generalized medium with finite bandwidth, additive noise and delay in the communication channel (Eisencraft *et al.* 2012), medium with multi-path propagation, noise and chaotic interference (Baptista 2021), and some other media. In the latter study, Baptista reports the preservation of the largest Lyapunov exponent of a chaotic signal when it propagates in a medium, which is a strong argument for further development of CCS.

In our previous work (Rybin *et al.* 2023), we presented the practical implementation of CCS based on a 32-bit microcontroller. The signals in this system were transmitted through a wire, and considered disturbances included only additive white Gaussian noise. In the current study, we attempt to implement coherent CCS in an audible acoustic channel, which primarily assumes frequency-dependent dissipation and attenuation. The novelty and contribution of the study are as follows.

1. We identify the acoustic channel and then optimize the frequency and data transfer rate of the chaotic generators to better match physical channel properties.

2. The original mechanism to counteract signal attenuation is proposed, namely, normalization of the received signal to levels that corresponds to undisturbed signals generated by oscillators with the appropriate parameter sets.

3. By computer simulation and hardware-in-the-loop (HIL) implementation of the developed CCS, which uses physical acoustic path, we study bit error rate, transfer rate, and security of the designed communication system and draw conclusions about the necessity of signal pre-filtering and bit error correction mechanisms.

The paper is organized as follows: in Section 2, the description of the modulation scheme and hardware is provided, as well as the basic chaotic oscillator and secrecy estimate. Section 3 presents the results of the simulation and experimental investigation of the designed CCS prototype. Section 4 discusses obtained results and concludes the paper.

MATERIALS AND METHODS

Sprott Case S system and its parameterization

In 1994 J. Sprott found a number of simple chaotic systems in the form of third-order ordinary differential equations (Sprott 1994) that possessed different attractor topologies in the presence of only one kind (multiplication). The Case S is an attractor possessing one unstable saddle equilibrium position and remaining chaotic over a wide range of parameters, with its largest Lyapunov exponent in the large region of the parameter space where the chaotic dynamics is observed exceeding that of the other Sprott systems. This implies a rapid exponential divergence of trajectories, which is useful for generating a broadband noise-like signal. The Case S system equations can be written as

$$\begin{cases} \dot{x} = -x - ay \\ \dot{y} = x + z^2 \\ \dot{z} = b + x \end{cases} \tag{1}$$

With typical parameters ($a \approx 4, b \approx 1$), the maximum Lyapunov exponent for Case S is about 0.18, indicating a chaotic state. Unlike analog circuits, the system is easy to implement numerically, which was used in the study of digital direct chaotic communication. The Sprott S system is of special interest for communications because it remains chaotic even with coarse sampling. In addition, its chaotic oscillations have a complex spectral composition and a wide frequency range.

The investigation of dynamical behavior in the Sprott Case S system was conducted through a multi-parameter analysis combining bifurcation diagrams and Lyapunov spectrum to evaluate transitions between periodic and chaotic regimes under parameter variation. Simulation was performed using both 4-th order Ruge-Kutta and 2-nd order semi-implicit CD (Butusov *et al.* 2019; Rybin *et al.* 2025) methods to verify the absence of numerical artifacts. A two-dimensional bifurcation diagram (Fig. 1a) was calculated by varying parameters a and b, revealing intricate structures of periodic windows embedded within chaotic regions. Additionally, the corresponding Largest Lyapunov exponent estimation (Fig. 1b) provided quantitative insights into the system's sensitivity to initial conditions, with positive values of λ_1 delineating chaotic domains. To isolate the influence of parameter a, one-dimensional bifurcation diagram (Fig. 1c) and Lyapunov spectrum (Fig. 1d) were calculated by replacing parameter b by the linear relationship $b = f(a) = 0.0602a + 0.7308$, derived from the dashed trajectory in Figures 1a-b.

This parametric substitution enabled targeted exploration of dynamical transitions along specific parameter pathways, revealing abrupt period-doubling cascades and crises indicative of chaos emergence. Further, we will consider the single-parameter Sprott Case S oscillator:

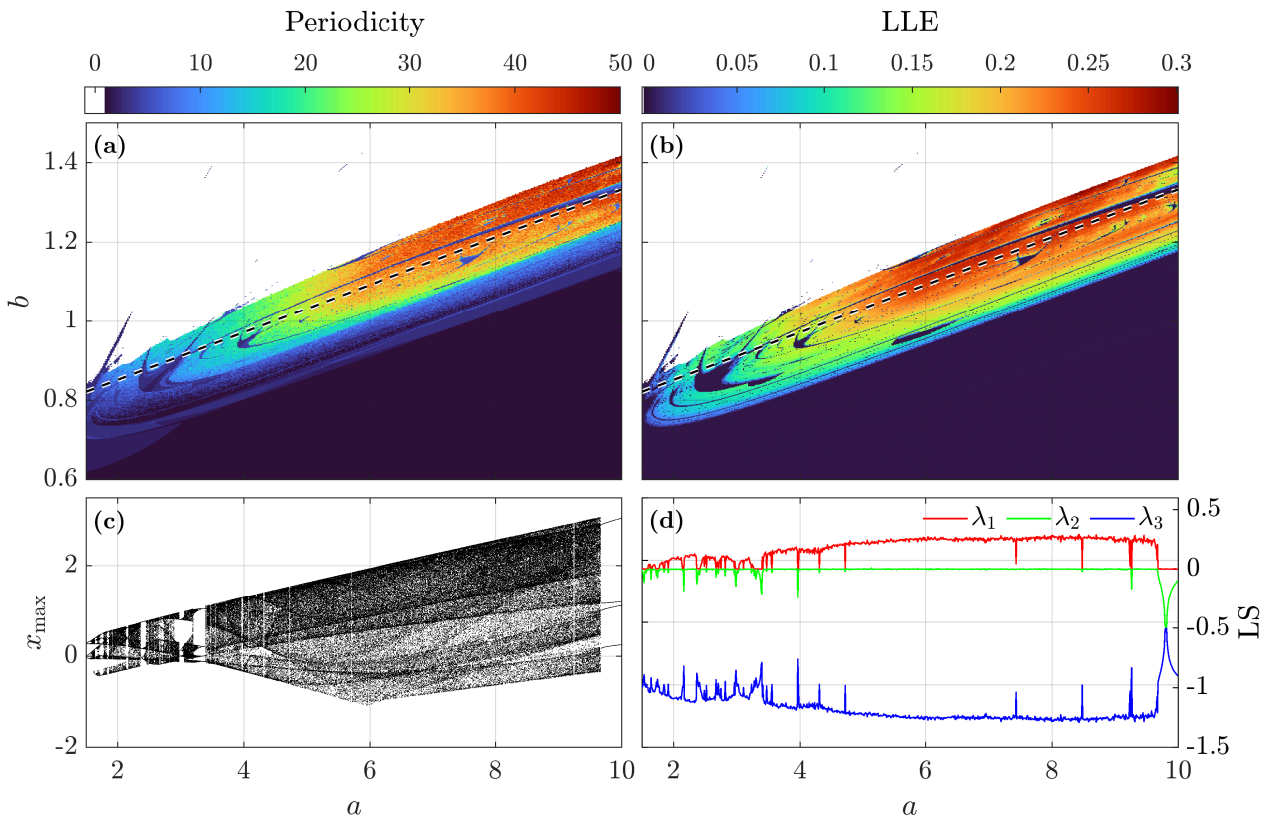

Figure 1 2D-Periodicity **(a)** and largest Lyapunov exponent **(b)** diagrams for Sprott Case S system, white color corresponds for unbound solution, black-white dash line corresponds for $b = f(a) = 0.0602a + 0.7308$. 1D-bifurcation **(c)** and Lyapunov spectrum **(d)** diagrams are calculated by varying parameter a with replacing parameter b by $f(a) = 0.0602a + 0.7308$.

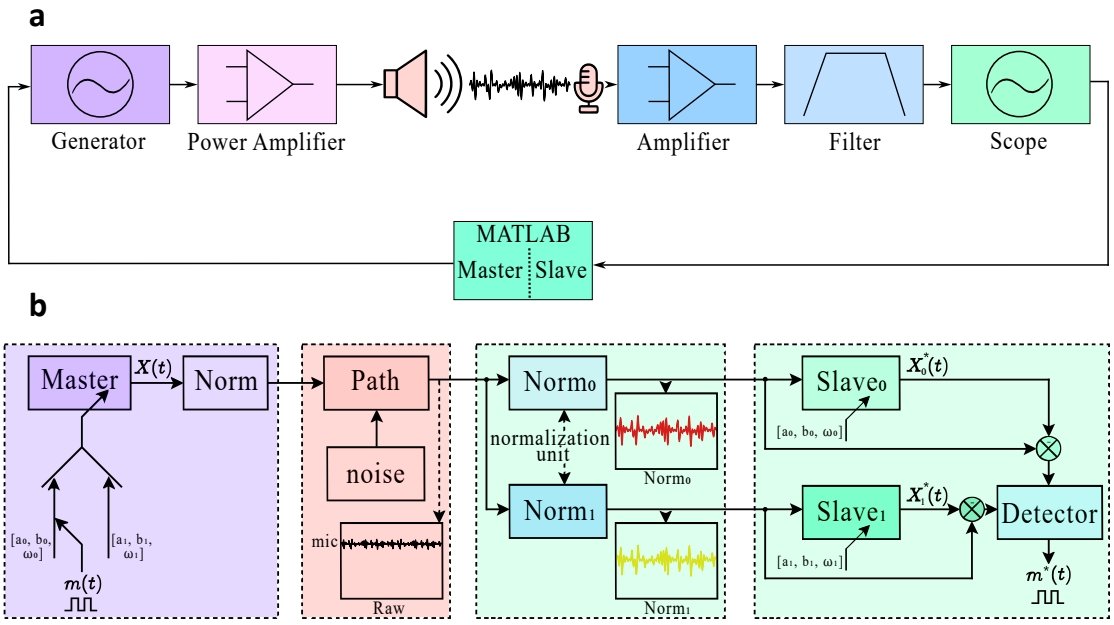

Figure 2 Schematic of the chaotic communication system with acoustic path. **a** Hardware-in-the-loop experiment with acoustic path implemented using physical devices, while receiver and transmitter are simulated in MATLAB; **b** detailed schematic of the communication system. The blocks of signal normalization set the waveform received from the path to those amplitudes and shifts, which correspond to the chaotic signals of system with given parameters

$$\begin{cases} \dot{x} = -x - ay \\ \dot{y} = x + z^2 \\ \dot{z} = 0.0602a + x + 0.7308 \end{cases} \tag{2}$$

Adaptation of chaotic system for non-ideal channel

Schematic of the proposed chaotic system and experiment is presented in Figure 2. For the acoustic channel research, a hardware-in-the-loop system was designed and implemented using a digital generator, speaker, microphone, and oscilloscope with signal recording functionality. As an audio frequency amplifier (AFA), a class D device based on chip TPA3118 is used, providing acoustic power up to 30 W per channel with a very low harmonic distortion. The observed distortion in the channel is caused by the small-sized speaker and, to a lesser extent, by low-cost piezoelectric microphone. The mic signal is pre-processed by an electric circuit based on MAX4466 amplifier.

The acoustic channel was measured by scanning with harmonic signals that cover the entire bandwidth, with synchronous recording of the emitted and received signals. In the subsequent automated processing of the experiment, noise multiplicative interference in the received signal was taken into account. The received signal was recorded from the output of the microphone amplifier as it was then fed into an analog or digital chaotic system as a synchronization signal. The Keysight Technologies 33210A signal generator was used to construct signals, and Rigol DS1104 four-channel digital oscilloscope was used for recording. As a result, frequency response of the channel $H(f_k)$ for the frequencies f_k was obtained.

Simulation of the channel was carried out using the signal $x(t_n)$ decomposition by fast Fourier transform, multiplication of the spectrum by the channel frequency response $\widetilde{H}(f_n)$ interpolated to a given frequency grid f_n, as only values for $H(f_k)$ are known, $f_n \neq f_k$, followed by the inverse Fourier transform to get signal in time domain. Notation t_n stands for discrete time $t_n = h \cdot n$, where $h = \Delta t$ is a time step, and n is the number of discrete sample.

$$X(f_n) = \mathcal{F}\{x(t_n)\} = \sum_{n=0}^{N-1} x_n \cdot e^{-j\frac{2\pi}{N}kn}, \quad k = 0, \ldots, N-1$$
$$Y(f_n) = X(f_n) \cdot \widetilde{H}(f_n),$$
$$y(t_n) = \mathcal{F}^{-1}\{Y(f_n)\} = \frac{1}{N}\sum_{k=0}^{N-1} Y_k \cdot e^{j\frac{2\pi}{N}kn}, \quad n = 0, \ldots, N-1$$

Mathematically, such transform is equivalent to the convolution of the signal $x(t)$ with impulse response of the path $h(t)$.

$$y(t_n) = x(t_n) * h(t_n)$$

The developed model was used to test propagation of Sprott Case S signal through the acoustic media.

To adopt the chaotic system oscillations frequency to the frequency range of the path, an acceleration coefficient ω is introduced:

$$\dot{\mathbf{x}} = \omega f(\mathbf{x})$$

With that, master-slave synchronization of systems (2) would be as follows:

$$\begin{cases} \omega^{-1}\dot{x_m} = -x_m - ay_m \\ \omega^{-1}\dot{y_m} = x_m + z_m^2 \\ \omega^{-1}\dot{z_m} = 0.0602a + x_m + 0.7308 \end{cases}$$
$$\begin{cases} \omega^{-1}\dot{x_s} = -x_s - ay_s \\ \omega^{-1}\dot{y_s} = x_s + z_s^2 \\ \omega^{-1}\dot{z_s} = 0.0602a + x_s + 0.7308 + k(\tilde{z}_m - z_s) \end{cases} \tag{3}$$

Here, k is a synchronization coefficient, and $\tilde{z}_m$ is the master drive signal. If no channel is considered, $\tilde{z}_m = z_m$, otherwise $\tilde{z}_m = f_{path}(z_m)$, where f_{path} is a function which distorts the master signal. For the channel simulation, we use a combination of channel distortion with additive noise:

$$\tilde{z}_m(t_n) = z_m(t_n) * h(t_n) + \epsilon_{0,\sigma^2} \tag{4}$$

where ϵ_{0,σ^2} is an additive white Gaussian noise.

To estimate the effect of the channel model on the chaotic signal, the spectral difference Δ_f between two instancies of the chaotic signal before and after propagating through the channel may be estimated:

$$\Delta_f = RMS(\tilde{Z}_m(f_n) - Z_m(f_n)).$$

As another estimate, close to the practical operation of a coherent communication system, the RMS error of synchronization of two chaotic oscillators can be taken. Note that the distorted master signal is used to calculate the synchronization error, since the exact value of this signal is unknown at the receiver side.

$$\Delta_{t_n} = RMS(\tilde{z}_m(t_n) - z_s(t_n)).$$

Using the proposed approach, the optimization of Case S to frequency properties of the propagation path was performed, see Figure 3.

The results in Figure 3 show the consistency of both metrics Δ_{t_n} and Δ_f. The figure shows that there exists the range of parameters ω, for which the synchronization between master and slave systems has the lowest error. In this range, the distortion of the master signal spectrum is also minimal. Here and further, values of syncrhonization coefficients $k_0 = 4.6$ and $k_1 = 5.7$ were used for Slave 0 and Slave 1, respectively.

As the optimal value, $\omega^* = 2.6 \cdot 10^3$ was taken. This value is not the exact mathematical optimum but is accurate enough considering the inevitable discrepancy between model and real path and also may be varied, keeping synchronization at an acceptably fine level (we will use this option further). For a different chaotic system and a different physical path, the optimal ω value will differ, but the search procedure will be similar.

Modulation and demodulation

At the transmitter side: we use chaotic system parameters modulation to encode binary symbols '0' and '1'. Symbols are presented as parameter vectors $\mathbf{p}_0$ and $\mathbf{p}_1$, which may include all the parameters: a, b (as a function of a) and ω. The need for the last parameter to be modulated is presented in Figure 4. For '0' and '1', $a_0 = 4.65$ and $a_1 = 6.1$ were chosen. One may see that although the spectrum for both parameters is generally similar, the specific peak frequency values are significantly different, which may be easily captured by spectrogram analysis, see Figure 5(a).

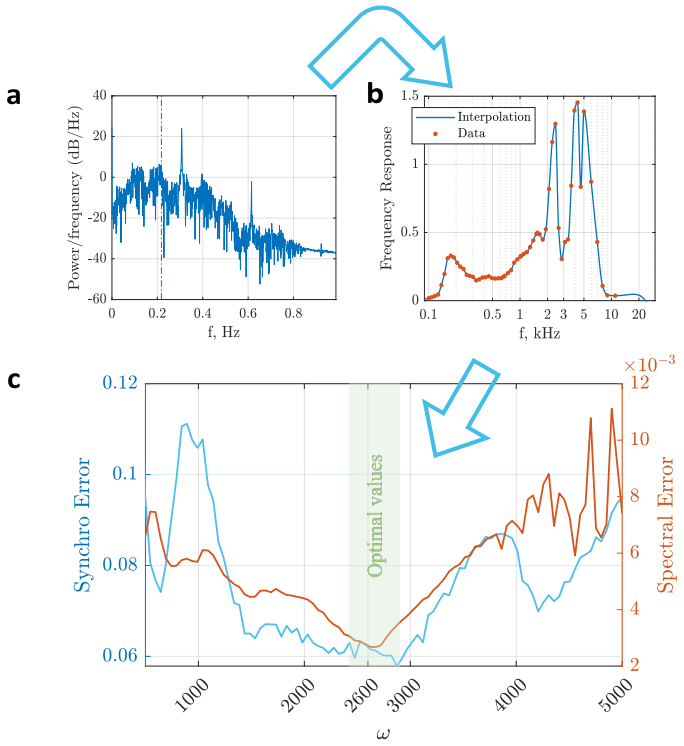

Figure 3 Optimization of parameter ω to find the best match between the channel frequency response and spectrum of Sprott Case S chaotic system: (a) Sprott Case S (2) spectrum, i.e. $\omega = 1$, (b) frequency response of the measured acoustic channel, (c) dependence of synchronization error between two identical chaotic oscillators when master signal was propagated through the channel Δ_{t_n}, and difference of spectra Δ_f between two instancies of chaotic signal before and after propagating through the channel, on ω.

Take the following parameter vectors: $\mathbf{p}_0 = [4.65, 1.11\omega^*]$ and $\mathbf{p}_0 = [6.1, 0.95\omega^*]$. In the first case, the median frequency of oscillations is increased, and in the second, decreased, to stay around optimal, feasible to the path frequency response. As a result, the data transmission becomes almost invisible for the spectral analysis, see Figure 5(b).

As presented in the schematic in Figure 2(b), each symbol waveform is normalized before being sent into a channel. The reason may be seen in Figure 1(c): the amplitude of the signal also changes with variation of a. Normalized waveforms are glued together using the cross-fade function to get smooth transitions between symbol waveforms.

At the receiver side: the signal is first re-normalized to return it back to the appropriate amplitude and shift equal to those of an undistorted signal. Before communication is established, these parameters are found numerically for each of the parameter vectors $\mathbf{p}_i$:

$$A_i = \max_{t\in[0,T]} |z(t)_i| \tag{5}$$

$$C_i = \frac{1}{T}\int_0^T z(t)_i\, dt \tag{6}$$

After reading input signal from the channel, the signal is normalized to $[-1, 1]$:

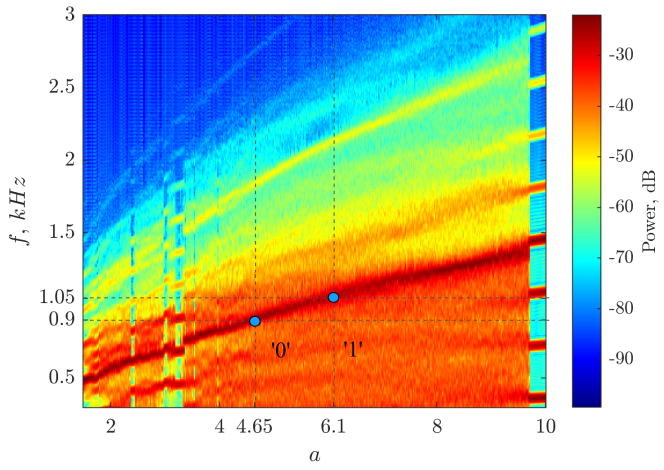

Figure 4 Bifurcation spectral diagram of Sprott Case S chaotic system adopted for physical channel with $\omega = 2.6 \cdot 10^3$.

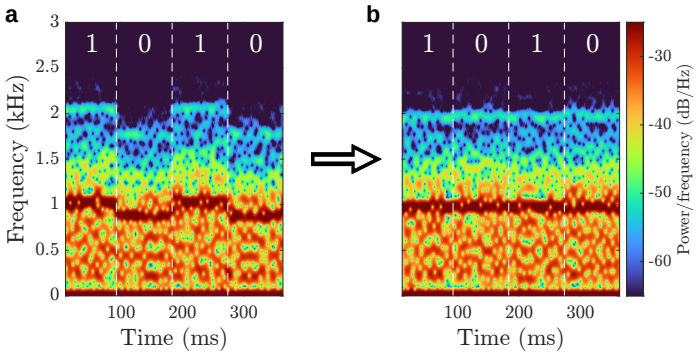

Figure 5 Spectrogram of the message '1010' transmitted before and after including ω in vector of modulated parameters.Spectrogram in **b** shows that spectral attack cannot be applied to decrypt the message.

$$z_{\text{norm}}(t) = 2 \cdot \left(\frac{z(t) - z_{\min}}{z_{\max} - z_{\min}}\right) - 1 \tag{7}$$

where $x_{\min} = \min x(t)$, $x_{\max} = \max x(t)$.

Then, the signal is amplified and shifted:

$$\tilde{z}(t)_i = A_i \cdot z_{norm}(t) + C_i \tag{8}$$

where A is the scale coefficient, C is the vertical shift.

The detector determines which of the two oscillators at the receiver side, with the parameter vectors $\mathbf{p}_0$ and $\mathbf{p}_1$, is more accurately synchronized with the input signal and decides which symbol is being transmitted. If the synchronization error exceeds a certain threshold, the detector recognizes this as the absence of a transmission in the channel.

Scheme of the experiment: is presented in Figure 2, relating the communication system to the broader class of chaotic shift keying systems. As is shown in block diagram, a Generator initiates the process by producing a signal generated previously in MATLAB software by master oscillator. The signal is then amplified through a Power Amplifier, transmitted using a Speaker, captured by a Microphone and further conditioned by a dedicated Amplifier.

This amplified signal passes through a Filter, likely designed to remove unwanted frequencies or noise, ensuring the signal meets the desired spectral characteristics. The filtered output is processed digitally by MATLAB software, where slave mathematical systems are simulated fed by this signal, and a message is decoded. The Master oscillator (labeled as $x(t)$) generates the primary signal, which undergoes parameters switching between sets (a_0, b_0, ω_0) and (a_1, b_1, ω_1). Then that signal is normalized and passed through a Path to Slave subsystems. The schematic references two Slave oscillators: Slave 0 and Slave 1, while demodulation is performed by analyzing synchronization errors on each of the slave oscillators.

Secrecy estimation

Quantified return map analysis (QRMA): is the further development of return map analysis (RMA), which has been widely used to attack chaotic communication systems. It was first demonstrated by Pérez and Cerdeira (1995) to extract messages masked by chaos. The method is that certain characteristic points (e.g., extrema) are extracted from the received chaotic signal and the dependence between their values is mapped. The resulting return transform reflects the dynamic properties of the chaos generator; a difference in the generator parameters (e.g., when transmitting 0 or 1) leads to a change in the type of return transform, which makes it possible to identify the transmitted bit. Nevertheless, the classical method of return transforms is qualitative: by visually distinguishing segments in the plane, it is clear that the parameters are changing. Until recently, there have been no reliable ways to quantify these differences, making it difficult to assess the level of secrecy and compare different chaos modulation methods in terms of security. However, without a quantitative measure, it is difficult to objectively judge the effectiveness of methods that are proposed to increase the complexity of return transform analysis. In this study, the distinguishability between chaotic signals is assessed by QRMA (Rybin *et al.* 2022) which is implemented as follows. For a given chaotic signal $x(t)$, local extrema (peaks X_m and valleys Y_m) are identified to compute recurrence points. These points form coordinates for the return map, which is discretized into an $N \times N$ grid to create a histogram matrix $H \in \mathbb{R}^{N\times N}$. To compare two signals (e.g., transmitted binary symbols), their histograms X and Y are analyzed using the formula:

$$\Delta_{i,j} = \|X_{i,j} - Y_{i,j}\| \cdot \|\Theta(X_{i,j}) - \Theta(Y_{i,j})\|, \quad i,j \in [1,N],$$

where Θ is the Heaviside step function and $\epsilon \in \mathbb{N}$ acts as a noise threshold:

$$\theta(x) = \begin{cases} x & \text{if } x \geq \epsilon \\ 0 & \text{if } x < \epsilon \end{cases}.$$

The normalized difference metric D is calculated as:

$$D = \sum_{i=1}^{N}\sum_{j=1}^{N} \frac{\theta(\Delta_{i,j})}{\theta(X_{i,j}) + \theta(Y_{i,j})}.$$

This metric quantifies the percentage difference between signals, with higher values indicating distinguishable modulation.

Amplitude return maps, which rely on peak-valley amplitudes, are unsuitable for systems with amplitude distortions (e.g., hydroacoustic channels). Instead, phase return maps focus on interpeak/intervalley intervals, preserving frequency characteristics unaffected by amplitude noise. For phase return maps, intervals between consecutive peaks X_m and valleys Y_m are defined as:

$$W_{2,m} = T(X_m) - T(X_{m-1}), \quad U_{2,m} = T(Y_m) - T(Y_{m-1}),$$

where $T(\cdot)$ denotes the timestamp of an extremum. Symmetric coordinates are computed as:

$$A_{t,m} = \frac{W_{2,m} + U_{2,m}}{2}, \quad B_{t,m} = W_{2,m} - U_{2,m},$$

$$C_{t,m} = \frac{W_{2,m+1} + U_{2,m+1}}{2}, \quad D_{t,m} = U_{2,m} - W_{2,m+1}.$$

Plotting A vs. $-B$ and C vs. $-D$ generates the phase return map. This approach captures temporal dynamics, making it robust to amplitude distortions.

RESULTS

Simulation

Simulation of the proposed CCS was performed in MATLAB environment using Runge-Kutta 4-th order method and simulation time $h \approx 2 \cdot 10^{-5}$ (the particular value was chosen with respect to ω). For this task, a class called *ChaoticCommunication* was developed for keeping all the parameters of the simulated system, which included functions for simulation of all necessary steps, i.e.: preliminary system parameters estimation (e.g. scaling factors for further normalization), message waveform generation, path simulation, signal normalization at the receiver side, synchronization of slave oscillators with the normalized signal, message detection based on the synchronization error, messaging quality estimation, and spectral and return map analyses.

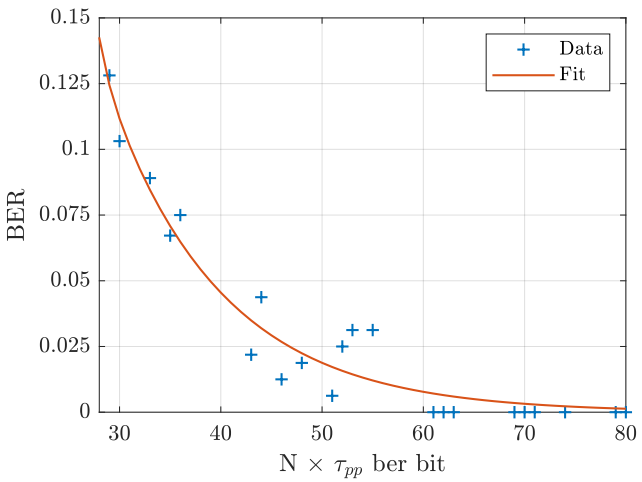

Figure 6 Estimation of bit error rate for different bit duration times. N denotes the duration in pseudo-periods (τ_{pp}).

To establish a stable difference between the transmitted bits in conditions of signal distortion, the transmission time of one bit was investigated. Figure 6 shows the dependence of the bit error rate (BER) on the length of the transmitted message. Simulation and analysis were performed for a number of 32-bit messages. Along the horizontal axis, the length of the transmitted bit is shown in pseudo-periods $\tau_{pp} = f_{mean}^{-1}$. One can see a local minimum around the transmitted bit length of 50 pseudo-periods, which means that some 32-bit messages can be transmitted without errors at the transfer rate of 11 bit/sec, see Figure 7 for an example. For Sprott Case S and $\omega = 2.6 \cdot 10^3$ approximately $t_{bit\,duration} \approx$ 90 ms, which results in a sample rate of 11 bit/sec, which is a feasible rate for implementations based on microcontrollers (Rybin *et al.* 2023). However, from Figure 6 it follows that a bit duration

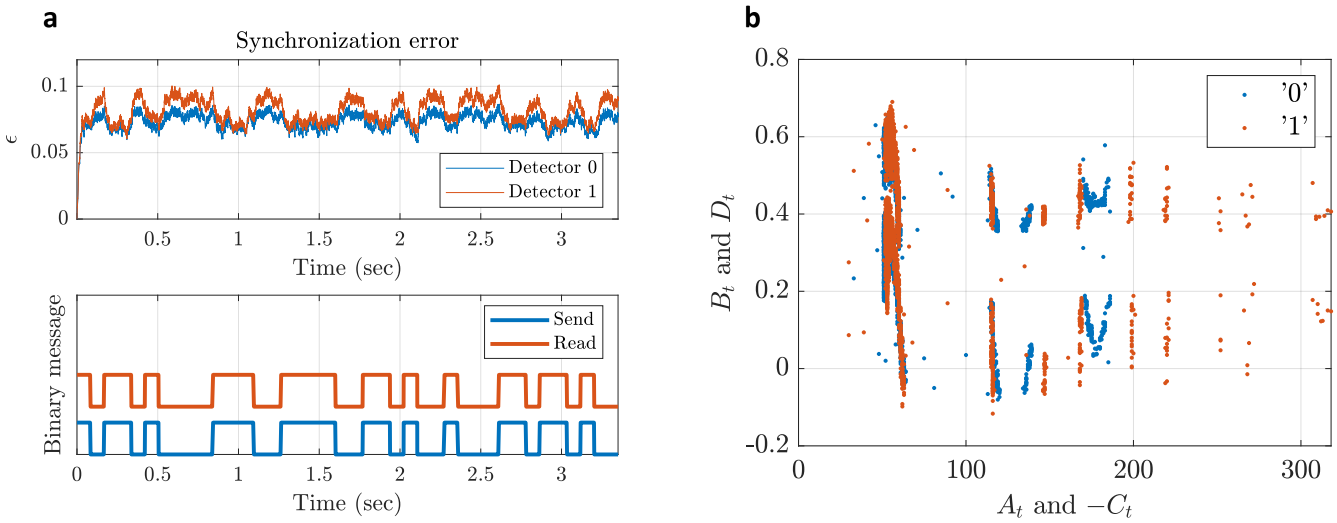

Figure 7 Simulation data on the chaotic communication system with acoustic path. **a** Synchronization error and binary messages (sent and received) for the communications simulated in MATLAB with bit duration $50 \times \tau_{pp} \approx 90$ ms. The relative synchronization error between '0' and '1' for $t_{bit\,duration} = 50\tau_{pp}$ is about 16%. **b** Estimation of amplitude-phase QRMA in simulated path: $\Delta_{0,1} = 12\%$

of at least 80 pseudo-periods must be taken to establish reliable communication. With the established parameters of the designed acoustic communication system, this results in message rates below 7 bits/sec.

Experiment

The experiment was set up as follows. The waveform with the embedded message was generated in MATLAB and then written to a CSV file. This file was then read by an arbitrary waveform generator and played back in real time. The signal from the generator was fed to a power amplifier driving the speaker. The acoustic signal from the speaker was picked up by a chip-based microphone module with a preamplifier and then recorded on an oscilloscope in CSV file. This file was then read by MATLAB, and the recorded signal was substituted for the computer-generated one when simulating the communication system.

The photograph of the experiment, as well as the results of the message transmission and comparison of the frequency response between simulated and real path are presented in Figure 8. Particular models of the hardware items used are listed in the caption.

According to the experimental results, e.g., comparison of the synchronization error and the QRMA plot, we may conclude that the real path presents noticeably greater difficulties in establishing reliable communication than in the simulation. In particular, the synchronization error in the real path is almost two times higher. At the rate of 11 bit/sec, long messages were not successfully transmitted without error, but we observed messages of 8 bits length transmitted without errors.

Comparison in the terms of secrecy

Table 1 summarizes the key properties of the CCS with developed modulation technique and without introduced enhancements. The experiments were carried out using simulation of the proposed chaotic communication system based on Sprott Case S oscillator. Comparison with other works known from the literature may be irrelevant due to the variety of algorithms used to evaluate secrecy (if they are ever applied). Recent works applying some estimates of the chaotic communication systems secrecy include: Mushenko *et al.* (2020); Bonny *et al.* (2023); Babkin *et al.* (2024); Bonny and Al Nassan (2024); Rybin *et al.* (2025), etc. One may note that estimates are often proposed in graphical rather than numerical form, e.g. in the form of return maps, histograms, and autocorrelation plots. Also, none of the mentioned works consider physical communication channel.

DISCUSSION

The key finding of this study is that even in conditions of strong nonlinear distortion of the transmitted signal in a direct chaotic communication system, it is possible to select transmitter parameters that would form an attack-resistant communication system utilizing simple Pecora-Carroll synchronization technique. Meanwhile, the current study just partly highlights the issues that need to be solved towards creating a practically applicable direct chaotic communication system.

Limitations: of the study are related to the fact that the demonstration of the system's operation is performed for one chaotic system and one set of parameters. The dependence of communication quality on distance between transmitter and receiver, as well as the influence of different types of physical channels and interferences on communication quality were not addressed. We believe that our results open a wide field for further research. Although in our example the communication system was possible to operate with a signal directly received from a path, signal restoration is desirable. In its simplest form, it may consist of denoising, which may be performed by various methods, including promising approaches, i.e., ensemble intrinsic time-scale decomposition (Voznesensky *et al.* 2022), synchronization with sequential cascade of slave oscillators (Butusov *et al.* 2018), etc. More sophisticated restoration methods may include the receiver signal convolution with reciprocal impulse response of the path, model-based identification and by using other approaches.

Practical implementation: of the proposed chaotic communication system should consider that one information symbol is transferred during several decades of pseudo-periods $\tau_{pp} = f_{mean}^{-1}$. Taking into account the Nyquist frequency, which should be at least 10 points

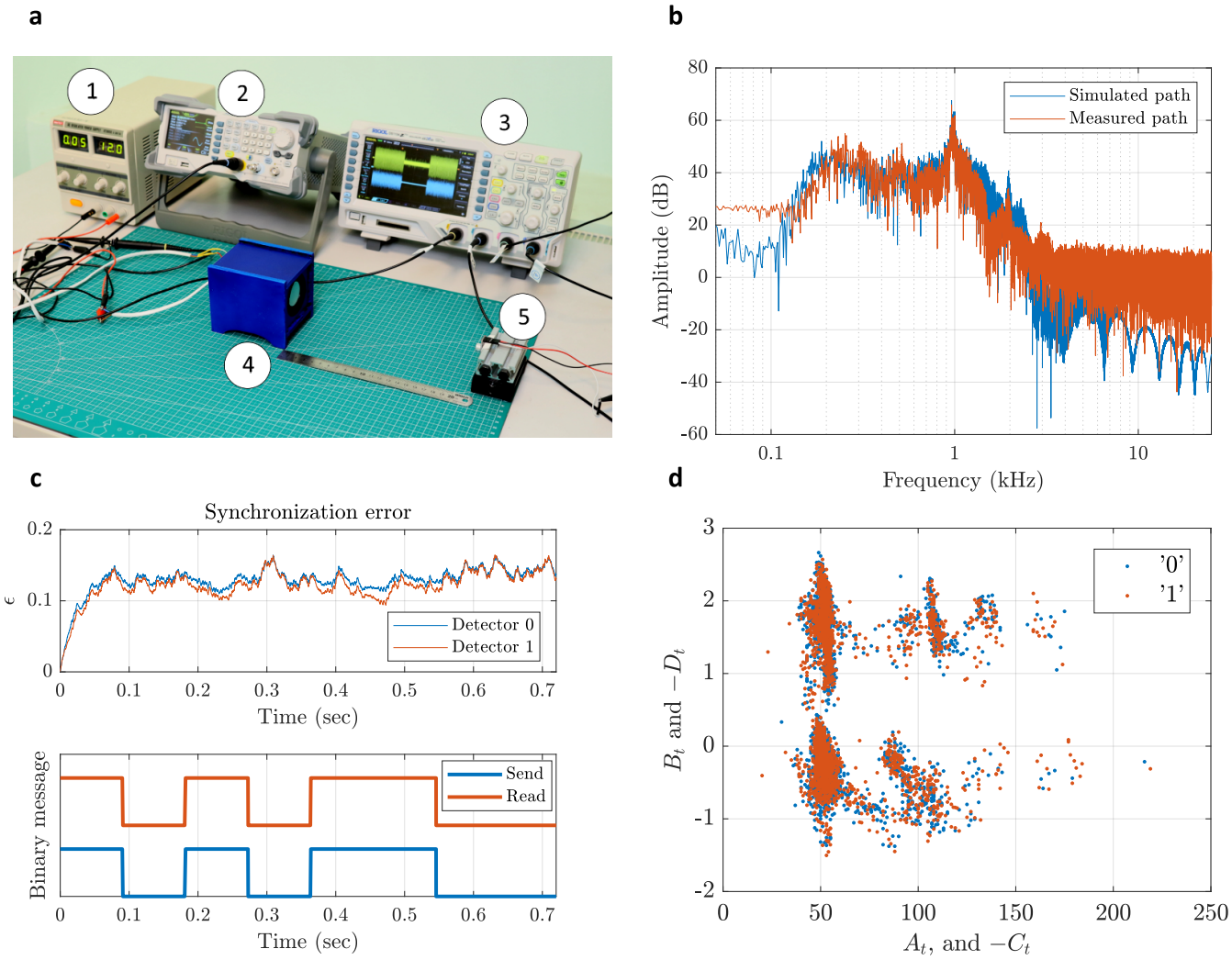

Figure 8 Experimental data on the chaotic communication system with acoustic path. **a** Photograph of the experiment. Here: (1) power supply for the amplifier of the speaker; (2) Rigol DG1032Z arbitrary signal generator reproducing the chaotic waveform with embedded message; (3) Rigol DS1054 oscilloscope used to capture both input of audio amplifier (yellow) and microphone output (blue) signals; (4) audio frequency amplifier based on chip TPA3118 and speaker in a single casing; (5) piezoelectric microphone with MAX4466 amplifier. **b** Spectra of the chaotic waveforms in simulated and measured paths. **c** Synchronization error and message waveforms for bit duration $50 \times \tau_{pp} \approx 90$ ms in physical acoustic path. The relative synchronization error between '0' and '1' for $t_{bit\,duration} = 50\tau_{pp}$ is about 7.5%. **d** Estimation of amplitude-phase QRMA in physical path: $\Delta_{0,1} = 5.2\%$.

Table 1 Secrecy estimates of chaotic communication system with proposed and standard modulation techniques

Vector of modulated parameters	References	Phase QRMA	Relative entropy difference between bits '0' and '1'	Pearson correlation between information message and energy in peak band (p-value)
$[a, b = f(a), \omega]$	This work	11.2%	1.09%	0.041
$[a, b = f(a)], \omega = 2.6 \cdot 10^3$	This work	67.5%	15%	0.53
$[a], b = 1.01, \omega = 2.6 \cdot 10^3$	Cuomo *et al.* (1993); Kaddoum (2016)	76.8%	17.3%	0.51

in the pseudo-period, the sampling rate of the system should be hundreds of times higher than the bitrate. Accounting for the need to use signal processing algorithms, FPGAs are the optimal digital platform for implementing direct chaotic communication systems.

Convergence issues are also to be considered when choosing the particular chaotic oscillator and sample rate. With that, utilization of fast time-reversible synchronization (Butusov *et al.* 2025) could significantly improve the transfer rate of coherent CCS, which also needs further study.

Applicability: of the proposed CCS in its current stage of development includes communication channels with moderate signal distortion and low to moderate transfer rates in which the information message must be disguised as noise. In underwater environments, this technology offers advantages in mitigating interference and minimizing ecological disruption with population-level consequences, particularly for animals with a limited geographic range (Trickey *et al.* 2022). E.g., it may be applied in navigation buoys and for short messages between the mothership and underwater self-acting robots.

CONCLUSION

In the current study, a new direct-chaotic communication system based on the Sprott Case S oscillator was proposed, which is characterized by high entropy values and a broadband noise-like signal providing high transmission security. One of the key features of the proposed system is the normalization block which aims to overcome signal attenuation in the physical channel. By optimizing oscillator dynamics, including tuning frequency scaling factor $\omega = 2.6 \times 10^3$, and modulation parameters $a_0 = 4.65$, $a_1 = 6.1$, we achieved synchronization stability and minimized spectral distortion, ensuring reliable data recovery and maintaining robust security. Experimental results show the applicability of the proposed approach for implementation in real-world physical applications with a relatively low data transfer rate of 7-11 bits/sec, which was demonstrated in a prototype. The Quantified Return Map Analysis (QRMA) revealed only 5-12% distinguishability between transmitted symbols, demonstrating a high level of secrecy.

This study bridges theoretical synchronization principles with practical implementation, validating coherent chaotic communication systems as a feasible alternative to conventional means in constrained environments. Future efforts to integrate advanced signal restoration and develop FPGA prototypes are still necessary steps towards practical application, but the current results solidify the foundation for chaos-based communication in real-world scenarios.

Acknowledgments

This study is supported by Russian Science Foundation, grant number 24-71-10064.

Ethical standard

The authors have no relevant financial or non-financial interests to disclose.

Availability of data and material

Not applicable.

Conflicts of interest

The authors declare that there is no conflict of interest regarding the publication of this paper.

LITERATURE CITED

Anishchenko, V., T. Vadivasova, D. Postnov, and M. Safonova, 1992 Synchronization of chaos. International Journal of Bifurcation and Chaos **2**: 633–644.

Babajans, R., D. Cirjulina, and D. Kolosovs, 2025 Field-programmable gate array-based chaos oscillator implementation for analog–discrete and discrete–analog chaotic synchronization applications. Entropy **27**: 334.

Babajans, R., D. Cirjulina, D. Kolosovs, and A. Litvinenko, 2022 Quadrature chaos phase shift keying communication system based on vilnius chaos oscillator. In *2022 Workshop on Microwave Theory and Techniques in Wireless Communications (MTTW)*, pp. 5–8, IEEE.

Babkin, I., V. Rybin, V. Andreev, T. Karimov, and D. Butusov, 2024 Coherent chaotic communication using generalized runge–kutta method. Mathematics **12**: 994.

Bai, C., H.-P. Ren, M. S. Baptista, and C. Grebogi, 2019 Digital underwater communication with chaos. Communications in Nonlinear Science and Numerical Simulation **73**: 14–24.

Baptista, M. S., 2021 Chaos for communication. Nonlinear Dynamics **105**: 1821–1841.

Bonny, T. and W. Al Nassan, 2024 Optimizing security and cost efficiency in n-level cascaded chaotic-based secure communication system. Applied System Innovation **7**: 107.

Bonny, T., W. Al Nassan, and A. Sambas, 2024 Comparative analysis and fpga realization of different control synchronization approaches for chaos-based secured communication systems. PLOS ONE **19**: 1–33.

Bonny, T., W. A. Nassan, S. Vaidyanathan, and A. Sambas, 2023 Highly-secured chaos-based communication system using cascaded masking technique and adaptive synchronization. Multimedia Tools and Applications **82**: 34229–34258.

Butusov, D., T. Karimov, A. Voznesenskiy, D. Kaplun, V. Andreev, *et al.*, 2018 Filtering techniques for chaotic signal processing. Electronics **7**: 450.

Butusov, D., V. Rybin, and A. Karimov, 2025 Fast time-reversible synchronization of chaotic systems. Physical Review E **111**: 014213.

Butusov, D. N., V. Y. Ostrovskii, A. I. Karimov, and V. S. Andreev, 2019 Semi-explicit composition methods in memcapacitor circuit simulation. International Journal of Embedded and Real-Time Communication Systems (IJERTCS) **10**: 37–52.

Cuomo, K. M., A. V. Oppenheim, and S. H. Strogatz, 1993 Synchronization of lorenz-based chaotic circuits with applications to communications. IEEE Transactions on circuits and systems II: Analog and digital signal processing **40**: 626–633.

Eisencraft, M., R. Fanganiello, J. Grzybowski, D. Soriano, R. Attux, *et al.*, 2012 Chaos-based communication systems in non-ideal channels. Communications in Nonlinear Science and Numerical Simulation **17**: 4707–4718.

Kaddoum, G., 2016 Wireless chaos-based communication systems: A comprehensive survey. IEEE access **4**: 2621–2648.

Kolumbán, G., G. Kis, Z. JaKo, and M. P. Kennedy, 1998 Fm-dcsk: A robust modulation scheme for chaotic communications. IEICE Transactions on Fundamentals of Electronics, Communications and Computer Sciences **81**: 1798–1802.

Mushenko, A., J. Dzuba, A. Nekrasov, and C. Fidge, 2020 A data secured communication system design procedure with a chaotic carrier and synergetic observer. Electronics **9**: 497.

Oppenheim, A., K. Cuomo, S. Isabelle, and G. Wornell, 1992 Signal processing in the context of chaotic signals . In *Acoustics, Speech, and Signal Processing, IEEE International Conference on*, volume 4, pp. 117–120, Los Alamitos, CA, USA, IEEE Computer Society.

Parlitz, U., L. CHUA, L. KOCAREV, K. HALLE, and A. SHANG, 1992 Transmission of digital signals by chaotic synchronization. International Journal of Bifurcation and Chaos **02**: 973–977.

Pecora, L. M. and T. L. Carroll, 1990 Synchronization in chaotic systems. Phys. Rev. Lett. **64**: 821–824.
Pérez, G. and H. A. Cerdeira, 1995 Extracting messages masked by chaos. Phys. Rev. Lett. **74**: 1970–1973.
Pisarchik, A., R. Jaimes-Reategui, and J. Garcia-Lopez, 2008 Synchronization of multistable systems. International Journal of Bifurcation and Chaos **18**: 1801–1819.
Rybin, V., I. Babkin, Y. Bobrova, M. Galchenko, A. Mikhailov, *et al.*, 2025 Variable-step semi-implicit solver with adjustable symmetry and its application for chaos-based communication. Mathematics **13**.
Rybin, V., D. Butusov, E. Rodionova, T. Karimov, V. Ostrovskii, *et al.*, 2022 Discovering chaos-based communications by recurrence quantification and quantified return map analyses. International Journal of Bifurcation and Chaos **32**: 2250136.
Rybin, V., T. Karimov, O. Bayazitov, D. Kvitko, I. Babkin, *et al.*, 2023 Prototyping the symmetry-based chaotic communication system using microcontroller unit. Applied Sciences **13**.
Sprott, J. C., 1994 Some simple chaotic flows. Phys. Rev. E **50**: R647–R650.
Trickey, J. S., G. Cárdenas-Hinojosa, L. Rojas-Bracho, G. S. Schorr, B. K. Rone, *et al.*, 2022 Ultrasonic antifouling devices negatively impact cuvier's beaked whales near guadalupe island, méxico. Communications Biology **5**: 1005.
Voznesensky, A., D. Butusov, V. Rybin, D. Kaplun, T. Karimov, *et al.*, 2022 Denoising chaotic signals using ensemble intrinsic time-scale decomposition. IEEE Access **10**: 115767–115775.
Wang, H., Z. zhi Han, and Z. Mo, 2010 Synchronization of hyperchaotic systems via linear control. Communications in Nonlinear Science and Numerical Simulation **15**: 1910–1920.
Wang, S., 2018 Dynamical analysis of memristive unified chaotic system and its application in secure communication. IEEE Access **6**: 66055–66061.

How to cite this article: Karimov, T., Mikhailov, A., Rybin, V., Sheptunova, V., and Butusov, D. Attack-Resistant Chaotic Communication System in Non-ideal Physical Channel. *Chaos and Fractals*, 2(2), 28-37, 2025.